Noninvasive control of stochastic resonance

John F. Lindner,[1,2] Jonathan Mason,[1] Joseph Neff,[1] Barbara J. Breen,[1] William L. Ditto,[3] and Adi R. Bulsara[4]
[1]*School of Physics, Georgia Institute of Technology, Atlanta, Georgia 30332-0430*
[2]*Department of Physics, The College of Wooster, Wooster, Ohio 44691-2363*
[3]*Georgia Tech/Emory Department of Biomedical Engineering, Atlanta, Georgia 30332-0535*
[4]*SPAWAR Systems Center, Code D364, San Diego, California 92152-5001*
(Received 22 September 2000; published 21 March 2001)

External feedback can enhance (or depress) the response of a noisy bistable system to monochromatic signals, significantly magnifying its natural stochastic resonance. We compare and contrast a variety of such feedback strategies, using both numerical simulations and analog electronic experiments. These noninvasive control techniques are especially valuable for noisy bistable systems that are difficult or impossible to modify internally.

DOI: 10.1103/PhysRevE.63.041107 PACS number(s): 05.40.−a, 05.45.−a, 02.50.−r

I. INTRODUCTION

Stochastic resonance (SR) is a nonlinear phenomenon that exploits background noise to enhance a system's response to a monochromatic signal [1]. Originally proposed as a potential mechanism for the occurrence of the terrestrial ice ages, SR has since been demonstrated in diverse experiments, involving physical, chemical, and biological systems [2]. Recently, Gammaitoni *et al.* [3] were able to *control* SR, so as to either suppress or enhance the output power at the signal frequency, by sinusoidally modulating the barrier height between the two wells of a bistable system. Unfortunately, in many systems of interest, such as neurons [4], it is difficult or impossible to modulate the relevant barrier (or threshold). Subsequently, Mason *et al.* [5] were able to enhance SR by adding *external* feedback that increases the likelihood of switching between states, thereby obviating the need to modify the system internally. Adopting a different approach, Rozenfeld, Neiman, and Schimansky-Geier [6] were able to enhance SR by superimposing dichotomic noise on the internal (background) broadband noise.

Here, we study a variety of external feedback techniques that modify SR and compare and contrast their strengths and weaknesses. In Sec. II, we review bistable SR and the general framework for our feedback and numerical techniques. In Sec. III, we examine various fixed amplitude binary feedback techniques, each of which can significantly enhance SR. We construct an analog electrical circuit to study one of these cases. In Sec. IV, we demonstrate that negative proportional feedback can also significantly boost SR. In Sec. V, we consider the effect of employing pulses of fixed duration. Although such pulses can increase the spectral power at the signal frequency, they actually depress SR. Section VI provides a theoretical framework to understand the enhancement mechanism, the effective reduction in the height of the potential barrier. Finally, in Sec. VII, we summarize our results.

II. FRAMEWORK

A. Controlled noisy bistable oscillator

The canonical example of SR involves a sinusoidally driven overdamped noisy bistable oscillator. Consequently, consider an oscillator evolving according to

$$m\ddot{x}+\gamma\dot{x}=-V'[x]+F_N[t], \tag{1}$$

where the prime denotes differentiation with respect to position and the overdots differentiation with respect to time. The oscillator's internal (background) noise engenders a stochastic force $F_N[t]=\sigma N[t]$, where $N[t]$ represents band-limited Gaussian white noise with zero mean and unit root-mean-square amplitude. The potential $V[x]=-\frac{1}{2}\alpha x^2+\frac{1}{4}\beta x^4$ is bistable provided $\alpha,\beta>0$. The choices $\alpha=32$ and $\beta=1$ establish a barrier of height $V_B=\alpha^2/4\beta=256$, of half width (or radius) $R_B=\sqrt{\alpha/\beta}=5.66$, and of maximum gradient (or maximum force) $F_B=\sqrt{4\alpha^3/27\beta}=69.7$. These parameters are used in our simulations. Because the regime of classical SR is overdamping, where viscosity dominates inertia $\gamma\dot{x}\gg m\ddot{x}$, we simplify the analysis by taking $\gamma=1$ and $m=0$.

To enhance the response of the oscillator described by Eq. (1) to monochromatic signals, we modify the system by adding a feedback controller $F_C[x]$, depending *implicitly* on time, so that

$$m\ddot{x}+\gamma\dot{x}=-V'[x]+F_N[t]+F_C[x]=-V'_{\rm eff}[x]+F_N[t], \tag{2}$$

where the effective potential $V_{\rm eff}=V-xF_C$. The goal of most of the feedback techniques presented here will be to effectively lower the barrier height of the potential.

Finally, to the modified system Eq. (2), noisy oscillator plus controller, we add a monochromatic signal $F_S[t]=A_S\sin[2\pi f_S t]$, so that

$$m\ddot{x}+\gamma\dot{x}=-V'_{\rm eff}[x]+F_N[t]+F_S[t]. \tag{3}$$

A weak signal amplitude $A_S=0.11F_B=8$ guarantees that the deterministic dynamics is typically subthreshold in the absence of the controller. Since signal amplitudes of $A_S\geqslant F_B$ effectively rock the potential so that its interwell barrier periodically disappears, the maximum force F_B is also known as the deterministic switching threshold, defined here strictly for dc or extremely slow modulating signals. For faster modulations, however, F_B still provides a reasonable approximation to the deterministic switching threshold.

B. Numerical techniques

We numerically integrate the stochastic differential Eq. (3) using a first-order technique [7] with a time step $\Delta t = T_S/2^{10} \approx 0.005$, where $T_S = 1/f_S$. We generate Gaussian noise using the Box-Muller algorithm [6] and a pseudo-random-number generator. The finite time step slightly correlates the noise by introducing an effective correlation time of $\tau = \Delta t/2$ and band-limits its spectrum to a Nyquist frequency $f_N = (1/2)\Delta t = 2^9 f_S \approx 100$. The noise intensity $D = \tau\sigma^2$ is the product of the correlation time and the variance.

From a long time series $x[t]$, we estimate the mean square amplitude per frequency, the power spectral density, or spectrum $S[f]$. Each spectrum consists of the magnitude squared of a normalized discrete Fourier transform [8]. To reduce the variance of the result, we typically average 2^{10} spectra each containing 2^5 periods of the signal. Sometimes, we first filter the time series so as to remove intrawell oscillation and focus on interwell hopping. (Specifically, before applying a fast Fourier transform algorithm to the time series, we replace every $x<0$ with -1 and every $x>0$ with $+1$.)

From a spectrum, we estimate the spectral response to the monochromatic signal by computing the dimensionless ratio $\rho = S[f_S]/\overline{S_0}$, where $S[f_S]$ is the spectrum at the signal frequency f_S (or the height of the spectral bin of width Δf centered on f_S), and $\overline{S_0}$ is the average of the spectrum near but not at the signal frequency f_S. This is conventionally expressed in decibels by the signal-to-noise ratio (SNR) $\mathcal{R} = 10 \log_{10} \rho$. This simple SNR definition [9] is appropriate because we want to quantify the response of the modified system Eq. (2), the controlled oscillator, to a *monochromatic* signal $F_S[t]$. Because $S[f_S]$ depends implicitly on the frequency resolution of the spectrum, we are careful to maintain a constant bin width $\Delta f = f_S/2^5$ throughout this study.

Figure 1 provides an example spectrum and SNR plot for an uncontrolled bistable oscillator. The spectrum consists of a sharp peak at the signal frequency superimposed on a smooth background [12]. (The slight rise in the high-frequency tail of the spectrum is an unavoidable aliasing artifact [8].) The SNR plot exhibits a local maximum at moderate noise, the signature of SR.

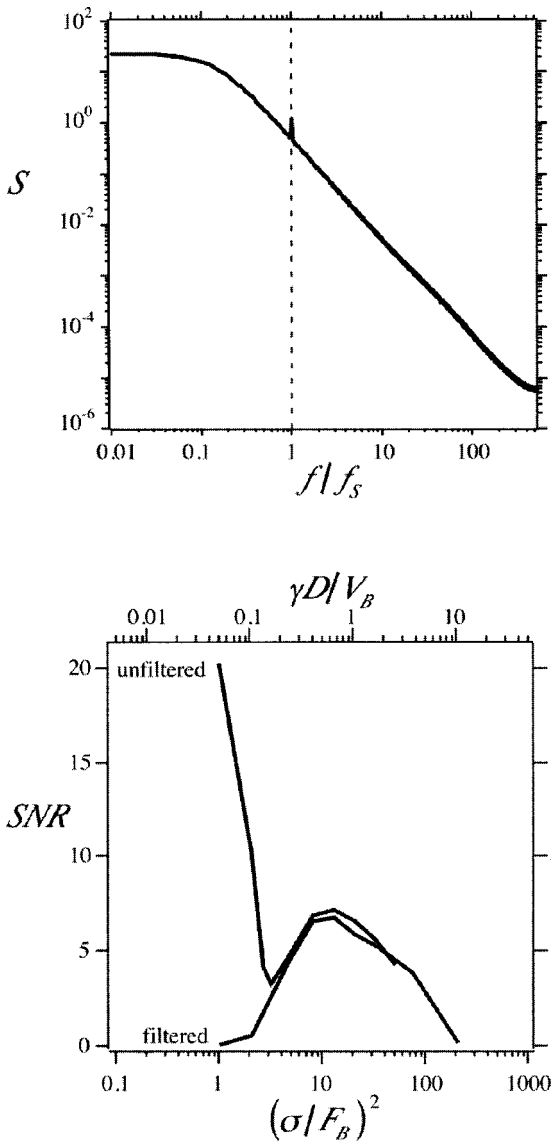

FIG. 1. Typical spectrum and SR plots for an uncontrolled bistable oscillator. Each spectrum $S[f]$ consists of a sharp peak at the signal frequency f_S superimposed on a smooth background. Each SNR, exhibits a local maximum at the resonant noise, whether the output is filtered (quantized) or unfiltered. The bistable potential has a barrier of height $V_B = 256$, radius $R_B = 5.66$, and hence maximum force $F_B = 69.7$. The signal has frequency $1/T_S = f_S = 0.195$ and amplitude $A_S = 0.11F_B = 8$.

III. FIXED AMPLITUDE FEEDBACK

A. Binary pulses

We first review the enhancement technique of Mason *et al.* [5]. Perhaps the simplest choice of controlling feedback with binary pulses so that

$$F_C[x] = -A_C x/|x| \tag{4}$$

If the oscillator is on the left side of the barrier, the controller pushes it to the right $F_C[x<0] = +A_C$, and, if the oscillator is on the right side, the controller pushes it to the left $F_C[x>0] = -A_C$. This effectively rocks the potential back and forth (nonperiodically) so as to encourage the oscillator to hop the central barrier. Indeed, the pulsed oscillator moves in an effective potential $V_{\text{eff}} = V - xF_C$ with a *lower* barrier height. (Interestingly, this effective potential is now tristable, with a cusp stable point at the origin.)

Figure 2 (top) displays the SNR versus internal (background) noise mean square amplitude σ^2, for a series of pulse amplitudes A_C. For low noise, there is only intrawell motion, which a filter eliminates, and the SNR vanishes. For moderate noises, each SNR exhibits a prominent local maximum, the signature of classical SR. Small to moderate pulse amplitudes $A_C \lesssim F_B$ cause the local maxima to drift to lower noises and higher values, culminating in a nearly 10 dB enhancement over the unpulsed SR. (Notice that the SNR increases at the location of the uncontrolled SR as well.) Very large pulse amplitudes $A_C \gg F_B$ destroy the SR by rendering

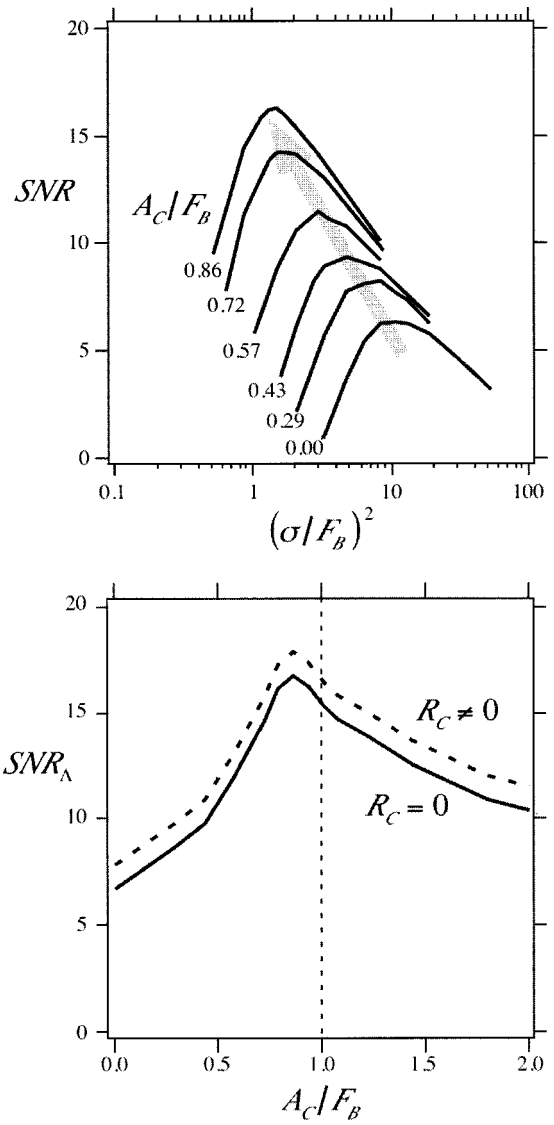

FIG. 2. Binary feedback enhances SR. Increasing the pulse amplitudes lowers the effective height and shifts the SR peak to lower noises and higher values. A pulse amplitude $A_C \sim F_B$ enhances the SR by about 10 dB. The dashed line on the bottom plot indicates the modest additional benefit of a small hysteresis threshold.

the interwell barrier insignificant and the potential effectively monostable, so that each SNR decreases monotonically with noise.

Figure 2 (bottom) displays the peak signal-to-noise ratio SNR_Λ as a function of pulse amplitude. Small to moderate pulse amplitudes $A_C \lesssim F_B$ cooperate with the internal (background) noise and with the signal to increase the SNR, and a pulse amplitude comparable to the maximum force provided by the potential $A_C \sim F_B$ maximizes the SNR. Slightly larger pulse amplitudes $A_C \gtrsim F_B$ degrade the SNR by stimulating the oscillator to hop the interwell barrier irrespective of the phase of the signal.

B. Binary hysteresis pulses

We experimented with adding a hysteretic threshold to the pulses to reduce the ''chatter'' in their application. Specifically, if $F_C = +A_C$ and the oscillator *increases* through $x = +R_C > 0$, then the controller resets $F_C = -A_C$; conversely, if $F_C = -A_C$ and the oscillator *decreases* through $x = -R_C < 0$, the controller resets $F_C = +A_C$. Adding a small hysteretic threshold $R_C = 0.1R_B$ improved the SR enhancement slightly (by an additional $\sim$2 dB). However, larger thresholds did not yield further improvements. The dashed line in Fig. 2 (bottom) summarizes these results.

C. Binary windowed pulses

We also experimented with adding a window outside which the pulses could be turned off. Triggered on by entering the interval (or window) $[-R_C, +R_C]$ from one side of the barrier, these pulses are shut off upon exiting the interval from the other side. This scheme might provide ''relief'' from the feedback for a sensitive system, such as a neuron. The tradeoff is that, the larger the window, the longer the pulses are on, and the better the enhancement; conversely, the smaller the window, the less the pulses are on, and the worse the enhancement. As the radius of the window decreases to zero $R_C \to 0$, we recover the SNR of the uncontrolled bistable oscillator. Figure 3 summarizes these results.

D. Analog experiment

We observed pulse enhanced SR experimentally in an analog electronic circuit for the binary hysteresis pulses of Sec. III B. Specifically, we constructed a circuit of passive elements (resistors, capacitors) and active elements (operational amplifiers or ''op amps''), whose voltage as a function of time mimics the position of the controlled sinusoidally driven noisy oscillator.

Figure 4 is a schematic of the circuit. The op amps with negative resistive feedback act as summing inverting amplifiers. The op amp with the negative capacitive feedback acts as an integrator. The op amp with positive feedback acts as a Schmitt trigger and implements the threshold hysteresis. Commercial wave generators supply the noise and signal. Kirchhoff's laws provide a differential equation for the voltage $V[t_E]$,

$$RC\frac{dV}{dt_E} = \frac{R_0}{R_1}V - \frac{R_0}{R_2}\mu^2\left(\frac{R_A}{R_B}+1\right)V^3 - \frac{R_0}{R_3}V_N[t_E] - \frac{R_0}{R_4}V_S[t_E] - V_P[t_E], \tag{5}$$

where, in addition to the resistances R_X and the capacitance C, μ is the proportionality constant of the multiplier integrated circuit, and t_E is the scaled time. Adjusting these parameters allows the amplitude dynamics to be scaled to fit the dynamic range of the discrete components while still allowing a direct comparison between simulation and experiment.

Figure 5 illustrates the experimental setup. The data acquisition (DAQ) system consists of a personal computer (PC) with a National Instruments PCI-MIO DAQ card and an AT-GPIB/NT general purpose interface bus (GPIB) card. A typical maximum sampling rate for the DAQ system is

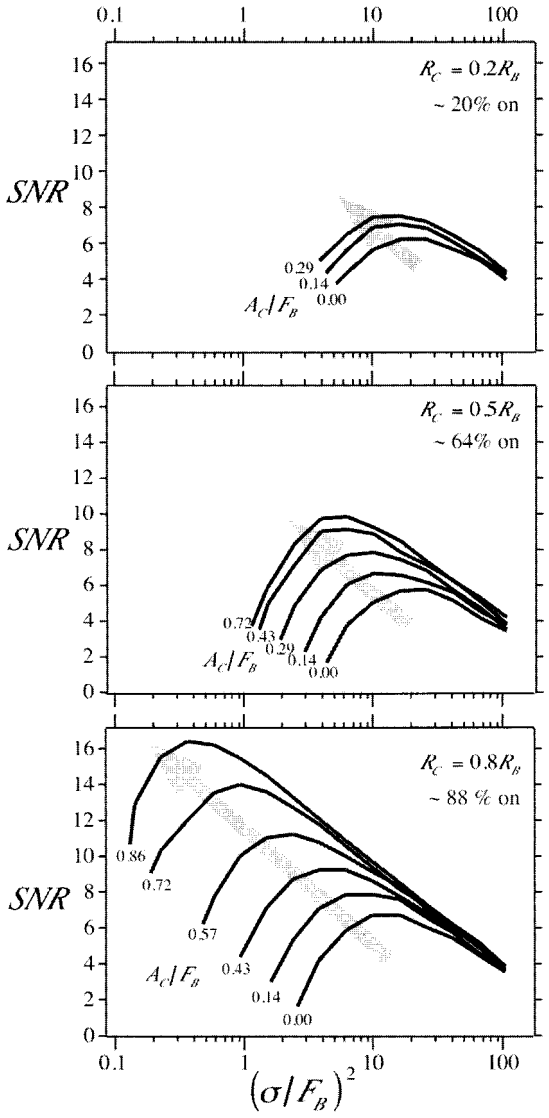

FIG. 3. Windowed binary feedback enhances SR, even when ''working'' part time. However, there is a tradeoff between ''time on'' and the degree of enhancement.

100/N kHz, where N is the number of recorded channels. The primary software package is LABVIEW 5.1, which is capable of controlling both the function generators, via the GPIB, as well as the DAQ card. This system can easily automate repetitive and lengthy measurements.

The primary job of the DAQ system is to make repeated time series measurements for a variety of parameter settings. The time series measurements are made at 32 768 Hz. The filter is set to low-pass the driving noise to 10 kHz. This ensures that the fastest frequency of the system is slower than the DAQ system's Nyquist frequency, which in this case is 16 384 Hz. Power spectra are calculated using the fast Fourier transform (FFT) algorithm. Because the period of the time series measurement and the period of the input frequency are commensurate, no windowing function is applied to the time series prior to the FFT. For each measurement of the SNR, 1000 power spectra are averaged. From the average output power spectrum the signal power at the driving frequency is measured and the background noise level is extracted using a curve fitting routine. The experimentally measured value of the SNR is $S/\Delta fN$, where S and ΔfN are the peak signal and background noise values, extracted from the power spectrum. The bandwidth is given by $\Delta f = f_s/N_s$, where f_s is the time series sampling frequency and N_s is the number of samples.

Figure 6 summarizes the experimental results. As the amplitude of the pulses increases, the SR moves to lower frequencies and higher values. This is in good qualitative agreement with the simulations.

IV. NEGATIVE PROPORTIONAL FEEDBACK

Another simple choice of controlling feedback is the restoring force

$$F_C[x] = -k_C x. \tag{6}$$

Because the mechanical force, derived from the true potential, is $-V'[x] = \alpha x - \beta x^3$, this feedback effectively renormalizes the potential's linear parameter $\tilde{\alpha} = \alpha - k_C$. Consequently, the relative height of the barrier $V_B/R_B = \sqrt{\tilde{\alpha}^3/16\beta}$ vanishes as $\tilde{\alpha} \to 0$, or equivalently as $\alpha \to k_C$. The vanishing of the barrier induces a sharp rise in the SR peak, until the local maximum in the SNR disappears near $k_C \sim \alpha$. Unfortunately, the SR peak also shifts toward lower noise, making it difficult to exploit the large SNR in the ambient noise of real environments. Figure 7 summarizes these results. (This strategy suggests yet another scheme, feeding back a *cubic* restoring force to linearize the effective potential.)

V. CONSTANT DURATION PULSES

Another possible control strategy is to apply fixed amplitude pulses of fixed duration. Triggered by a threshold crossing, such pulses automatically turn off after a fixed time. Specifically, if the oscillator enters the interval $[-R_C, +R_C]$ from $x < -R_C$, the controller adds a force $F_C = +A_C$ for a time T_C. Conversely, if the oscillator enters from $+R_C < x$, the controller adds $F_C = -A_C$ for a time T_C. Note that duration of the pulses T_C is also a ''refractory period;'' successive pulses are not allowed to overlap, even if the oscillator wanders in and out of the interval multiple times.

Constant duration control pulses (a near square wave pattern) introduce an extra frequency scale into the problem, namely, the inverse of the pulse duration. The corresponding power spectra now display a more complex sequence of interrelated peaks and dips, occurring at frequencies $mf_S \pm nf_C$ (m,n integers) [10,11]. For the case of a weak signal, dips appear in the spectrum $S[f]$ at the harmonics of the controller frequency f_C, as can be seen in the inset to Fig. 8 (bottom). The duration T_C controls the location of the main spectral peak. Adjusting T_C so that the peak coincides with the signal frequency f_S creates a local maximum in $S[f_S]$ but actually depresses the SR, as shown in Fig. 8. Since the total power is (approximately, under weak low-frequency driving) conserved in a bistable system [12], as power is increased in $f_C(A_C/F_B \to 1)$, one expects a renormalization and conse-

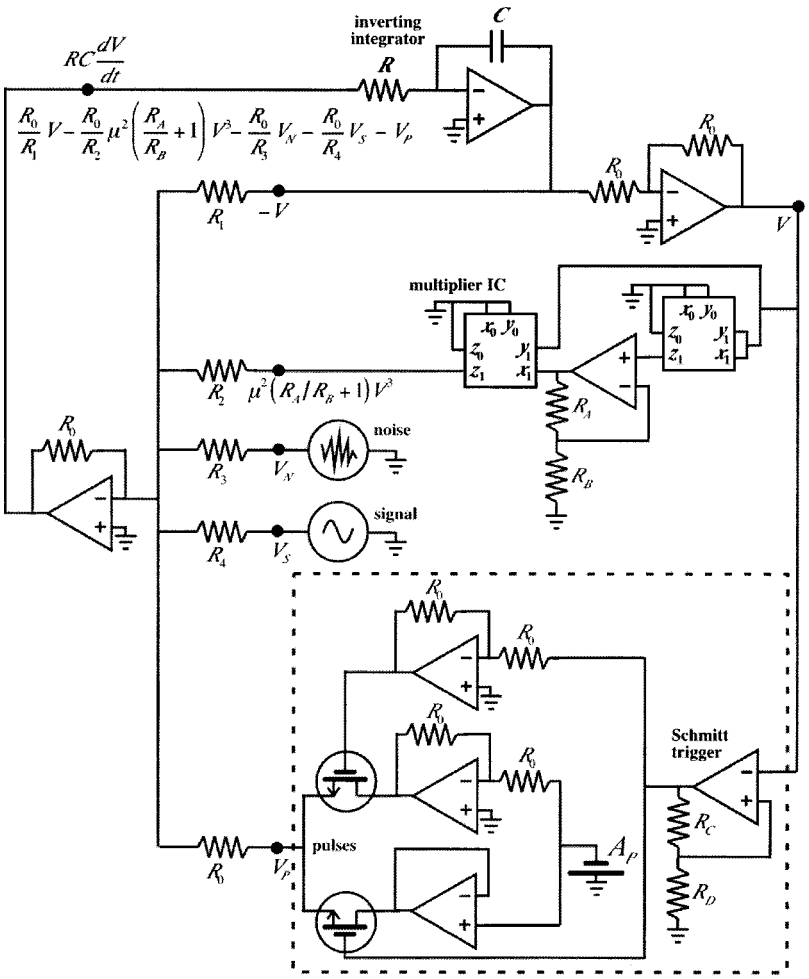

FIG. 4. Analog electronic circuit diagram that realizes binary feedback enhanced SR. The op amp with capacitive feedback acts as an integrator and the one with positive resistive feedback acts like a Schmitt trigger, while those with negative resistive feedback act as inverters, amplifiers, and an adder. The dotted box contains the controller, whose output is always $\pm A_C$.

quent decrease in power in the area under the peak for f_S [13]. This is particularly pronounced in the current scenario since the control signal is not a pure tone.

VI. THEORY

The essential mechanism of noninvasive control of SR is the effective reduction in the height of the barrier separating

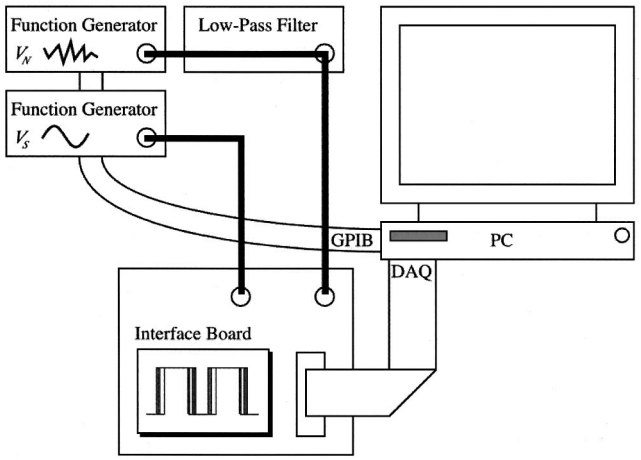

FIG. 5. Experimental data acquisition and control system for the analog circuit of Fig. 4.

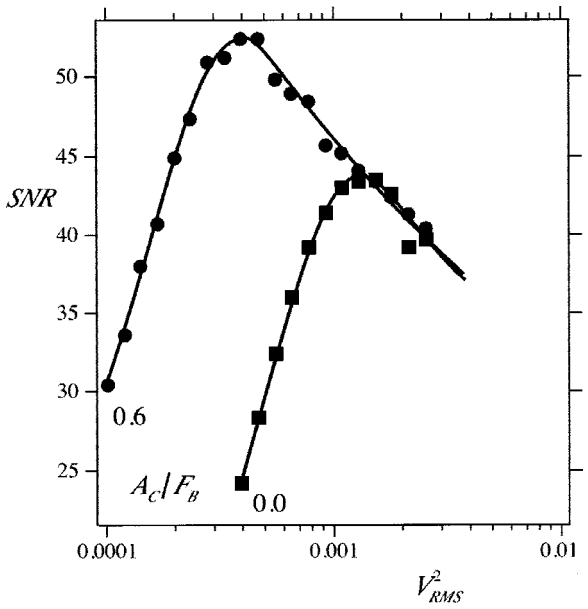

FIG. 6. Pulse enhanced SR in an analog electronic circuit. A pulse amplitude $A_C=0.6F_B$ shifts the circuit's SR peak to lower noises and higher values. The circuit mimics a bistable potential characterized by $V_B=128$, $R_B=5.66$, and hence $F_B=34.8$, while its signal is determined by $f_S=0.195$ and $A_S=0.29F_B=10$.

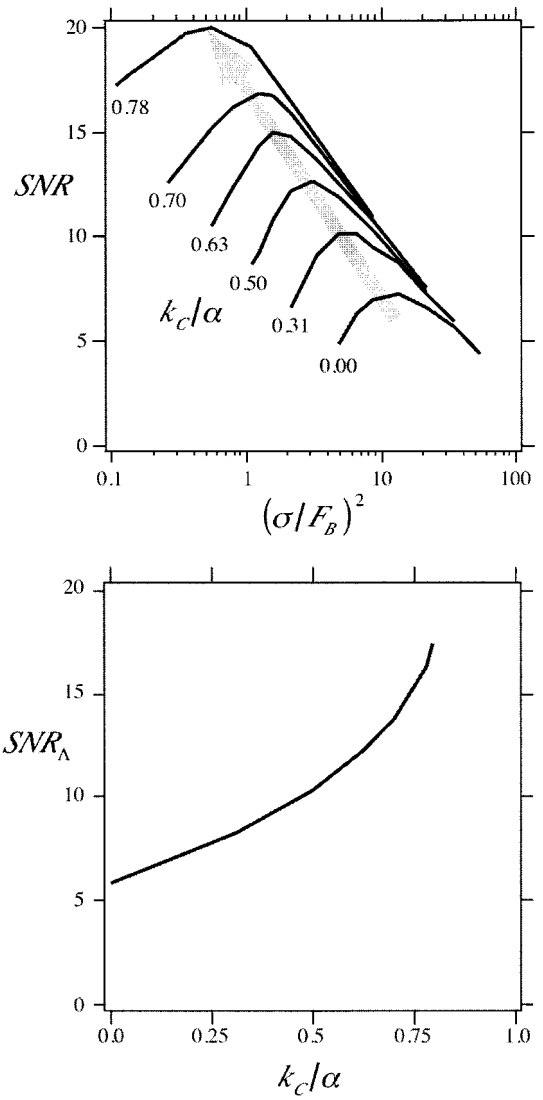

FIG. 7. Negative proportional feedback enhances SR until the SNR local maximum disappears as $k_C \to \alpha$. However, as the maximum SNR increases, it shifts to lower noise, making it more difficult to achieve in real, noisy environments.

the two wells of the bistable potential. Although the effective potential $V_{\text{eff}}=V-xF_C$ is not simple (for example, it contains a cusp for the binary pulses of Sec. III A), we may employ the McNamara-Wiesenfeld theory of bistable SR [12] to estimate the shift and rise of the SR peak with increasing pulse amplitude and decreasing effective barrier height.

If the signal is not too strong or too fast, then the mean time to hop the barrier can be approximated by Kramers' formula [14], which we write as

$$\tau_K \sim \pi\sqrt{2}\,\frac{\gamma R_B^2}{V_B}\exp\left[\frac{\gamma V_B}{D}\right]. \tag{7}$$

Substituting this into the resonant condition $\tau_K \sim 2T_S$, we solve for the resonant (or ''peak'') noise strength

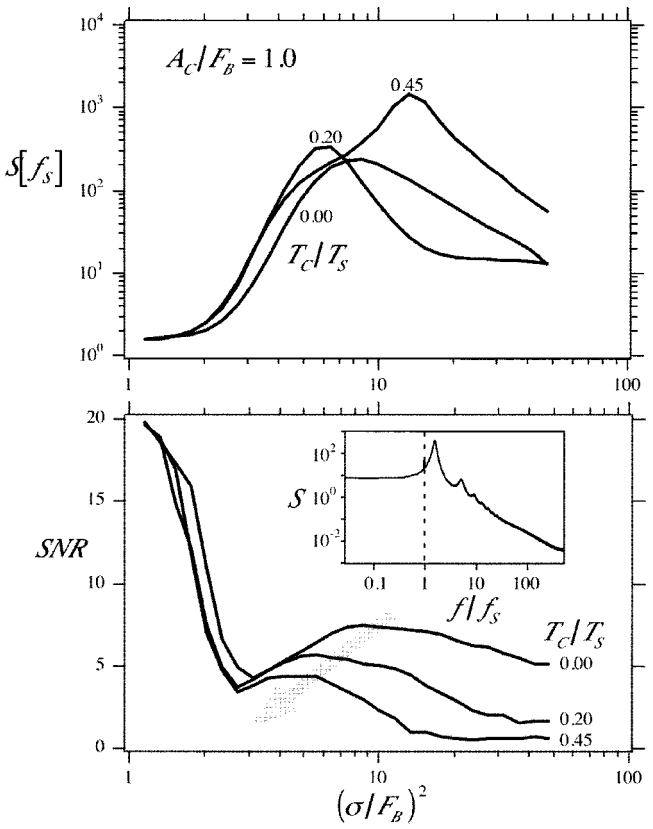

FIG. 8. Constant duration pulses can increase the spectrum at the signal frequency $S[f_S]$, if the duration is tuned appropriately, so that the fundamental spectral peak due to the approximate square waves of the pulses coincides with the signal frequency. However, this fundamental peak ''swallows'' the signal peak and *depresses* the SR. Inset depicts a typical spectrum $S[f]$.

$$D_\Lambda \sim \frac{2V_B\gamma}{\log_e[(\sqrt{2}/\pi)(V_B T_S/R_B^2\gamma)]}. \tag{8}$$

Similarly, if the signal is not too strong, then the spectral response $\rho = 1 + r/\Delta f$, where the ratio r is given by the McNamara-Wiesenfeld formula [12]

$$r \sim \sqrt{2}\,\frac{\gamma A_S^2 V_B}{D^2}\exp\left[-\frac{\gamma V_B}{D}\right]. \tag{9}$$

Substituting the resonant noise strength D_Λ given by Eq. (7), the resonant ratio r_Λ becomes

$$r_\Lambda \sim \pi\,\frac{A_S^2 R_B^2}{V_B^2 T_S}\log_e\left[\frac{\sqrt{2}}{\pi}\,\frac{V_B T_S}{\gamma R_B^2}\right]^2 \tag{10}$$

and so the resonant signal-to-noise ratio is $\text{SNR}_\Lambda = 10\log_{10}\rho_\Lambda = 10\log_{10}[1 + r_\Lambda/\Delta f]$.

Finally, we plot $\{\sigma_\Lambda^2, \text{SNR}_\Lambda\}$ parametrically as a function of the barrier height (or well depth) V_B. This theoretical result, which is indicated by the plot of Fig. 9, is in good agreement with the simulations. Notably, within its range of validity, it predicts that reducing the barrier causes the reso-

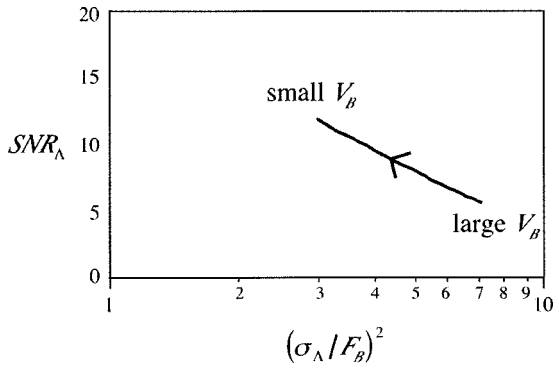

FIG. 9. Theory indicates that the SR peak should increase in value and shift to lower noise as the barrier height is progressively reduced.

nant SNR (the SR local maximum) to move to lower noise and higher values. Qualitatively, this behavior is plausible.

VII. CONCLUSION

An experimentalist can exploit a variety of simple feedback strategies to magnify a bistable stochastic resonance. Figure 10 graphically compares the strategies of SR enhancing controllers. Although the feedback depends on real-time monitoring of the time series, their structure (for example, $A_C \sim F_B$ for the binary pulses) depends only on the shape of the potential (and not at all on the frequency of the monochromatic signal), and hence may be determined before the experiment begins. Furthermore, these noninvasive techniques require only the application of *external* forces, rather than the *internal* modification of the potential, even as they effectively depress the interwell barrier.

Although these strategies have been developed for bistable SR, we expect that similar techniques can apply to threshold SR. Clearly, some modifications will be required, and the magnitude of the enhancement may differ. For example, since negative proportional feedback exploits the specific functional form of the bistable potential, this technique would obviously not have the same effect in a potential with a different analytical form or in a nonpotential threshold system, such as a neuron. However, insofar as neurons are bistable ''on-off'' systems, our general framework should apply. We hope to investigate such interesting generalizations in the near future.

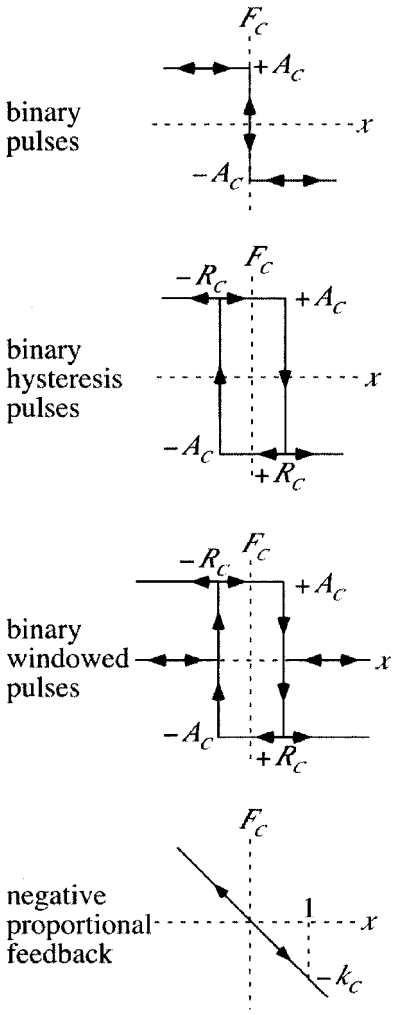

FIG. 10. A graphical summary and comparison of the SR enhancing control schemes. The arrows indicate the possible evolutions of the feedback control force $F_C[x]$.

ACKNOWLEDGMENTS

J.F.L. thanks The College of Wooster for making possible his sabbatical at Georgia Tech. W.L.D. acknowledge the Office of Naval Research, Physical Sciences Division for support. We thank Mark Spano and Kurt Wiesenfeld for helpful discussions.

[1] R. Benzi, A. Sutera, and A. Vulpiani, J. Phys. A **14**, L453 (1981); C. Nicolis and G. Nicolis, Tellus **33**, 225 (1981).

[2] K. Wiesenfeld and F. Moss, Nature (London) **373**, 33 (1995); A. R. Bulsara and L. Gammaitoni, Phys. Today **49** (3), 39 (1996); L. Gammaitoni, P. Hänggi, P. Jung, and F. Marchesoni, Rev. Mod. Phys. **70**, 223 (1998).

[3] L. Gammaitoni, M. Löcher, A. Bulsara, P. Hänggi, J. Neff, K. Wiesenfeld, W. L. Ditto, and M. E. Inchiosa, Phys. Rev. Lett. **82**, 4574 (1999).

[4] K. Wiesenfeld, D. Pierson, E. Panatazelou, C. Dames, and F. Moss, Phys. Rev. Lett. **72**, 2125 (1994); A. R. Bulsara, S. B. Lowen, and C. D. Rees, Phys. Rev. E **49**, 4989 (1994); P. Jung, *ibid.* **50**, 2513 (1994); H. Tuckwell, *Stochastic Processes in Neurosciences* (SIAM, Philadelphia, 1979).

[5] J. Mason, J. F. Lindner, J. Neff, W. L. Ditto, A. R. Bulsara, and M. L. Spano, Phys. Lett. A **277**, 13 (2000).

[6] R. Rozenfeld, A. Neiman, and L. Schimansky-Geier (unpublished).

[7] T. C. Gard, *Introduction to Stochastic Differential Equations* (Marcel Dekker, New York, 1988).

[8] W. H. Press, S. A. Teukolsky, W. T. Vetterling, and B. P. Flannery, *Numerical Recipes in C* (Cambridge University Press, New York, 1992).

[9] For response measures suitable for more general, nonmonochromatic inputs, consult, e.g., J. J. Collins, C. C. Chow, and T. T. Imhoff, Phys. Rev. E **52**, R3321 (1995); J. W. C. Robinson, D. E. Asraf, A. R. Bulsara, and M. E. Inchiosa, Phys. Rev. Lett. **81**, 2850 (1998); I. Goychuk and P. Hänggi, Phys. Rev. E **61**, 4272 (2000).

[10] J. W. S. Rayleigh, *The Theory of Sound* (Dover, New York, 1945) Vol. 2, Chap. 23.

[11] A. Grigorienko, P. Nikitin, and V. Roshchepkin, Zh. Eksp. Teor. Fiz. **85**, 628 (1997) [Sov. Phys. JETP **85**, 343 (1997)].

[12] B. McNamara and K. Wiesenfeld, Phys. Rev. A **39**, 4854 (1989).

[13] Since the canonical algorithm for computing the SNR defined above assumes a solitary frequency spike at the signal frequency superimposed on a *smooth* background, it can fail here dramatically. Although the eye may be able to pick out the small signal spike riding atop the peaks and valleys, it is difficult to fully automate this discrimination, especially in situations where the signal spike is very near a valley or peak. Fortunately, in this system, for small signal amplitudes, the *only* change in the spectrum due to the addition of a weak signal is a small spike at the signal frequency. Consequently, we estimate the background spectrum as $\overline{S_0} = S[f_S; A_S = 0]$ in computing the SNR.

[14] H. A. Kramers, Physica (Amsterdam) **7**, 284 (1940).